DOI: 10.1002/ejic.200900686

Magnetic and Electrochemical Properties of a Heterobridged μ-Phenoxido–$\mu_{1,1}$-Azide Dinickel(II) Compound: A Unique Example Demonstrating the Bridge Distance Dependency of Exchange Integral

Rajesh Koner,[a] Susanta Hazra,[a] Michel Fleck,[b] Arpita Jana,[a] C. Robert Lucas,*[c] and Sasankasekhar Mohanta*[a]

Keywords: Magnetic properties / Exchange interactions / Nickel / Schiff bases / Electrochemistry / Azides

The synthesis, structure, magnetic and electrochemical properties of the heterobridged μ-phenoxido–$\mu_{1,1}$-azide dinickel(II) compound $[Ni^{II}_2(HL^1)_3(\mu_{1,1}\text{-}N_3)]\cdot 3H_2O$ (**1**) derived from the tetradentate Schiff base ligand *N*-(2-hydroxyethyl)-3-methoxysalicylaldimine (H_2L^1) are described. The title compound crystallizes in the triclinic system (space group $P\bar{1}$). Electrochemical analyses reveal that compound **1** exhibits two-step quasireversible couples in the reduction window with $E_{1/2}$ values of –1412 and –1762 mV. The variable-temperature (2–300 K) magnetic susceptibilities at 1 T of the title compound were measured. The interaction between the metal centres is weak ferromagnetic (J = 5.0 cm^{-1}, g = 2.23, D_1 = 29.2 cm^{-1} and D_2 = 10.7 cm^{-1}). Comparison of the exchange integral of **1** with that of the only reported μ-phenoxido–$\mu_{1,1}$-azide dinickel(II) compound results in the emergence of a unique example of the dependence of strength of magnetic exchange interaction on the metal–ligand bridge distance.

Introduction

Molecular magnetism has been a frontier research area. Whereas discrete exchange-coupled systems are important to understand the nature and magnitude of exchange interaction and to determine magnetostructural correlations, large spin clusters and polymeric aggregates of interacting paramagnetic centres are important to develop molecule-based magnetic materials.[1–12] Regarding discrete systems, as most of the reported exchange-coupled compounds are antiferromagnetically coupled,[1] the designed synthesis of systems exhibiting ferromagnetic interaction is an important task.

It is known that few metrical parameters of the bridging moiety like bridge angle, dihedral angle between the basal planes and metal–ligand bridge distance may govern the nature and magnitude of exchange interaction.[1,2] To understand the absolute role of one parameter, other parameters should be constant for the related exchange-coupled systems. However, although such investigation is possible theoretically on fixing other parameters and varying one parameter,[12] it is quite difficult in the real systems to attain these criteria. If such a similarity can be attained for at least a pair of similar compounds, that should be an important observation in molecular magnetism.

Because of the involvement of two different bridges, the family of heterobridged exchange-coupled systems is considered as a special class in molecular magnetism.[1a,6–11] In contrast to the widely explored magnetic properties of heterobridged μ-hydroxido/alkoxido/phenoxido–μ-X (X = azide, thiocyanate, cyanate, pyrazolate, carboxylate, 7-azaindolate etc.) dicopper(II) compounds,[1a,2a,6] those of heterobridged compounds of other 3d metal ions[7–11] have been less investigated, and therefore, this area deserves more attention. It may also be noted that electrochemical properties of heterobridged systems are unexplored as well. However, the dependence of redox potentials and the stability of mixed valence species on the two different types of bridging moieties may result in interesting information.

With the anticipation that the combined effect of *N*-(2-hydroxyethyl)-3-methoxysalicylaldimine (H_2L^1; Scheme 1), obtained upon condensation of 3-methoxysalicylaldehyde with ethanolamine and a pseudohalide, may stabilize heterobridged systems, we have reported a rare example of a heterobridged μ-phenoxido–$\mu_{1,1}$-cyanate dinickel(II) compound $[Ni^{II}_2(HL^1)_3(\mu_{1,1}\text{-}NCO)]\cdot 2H_2O$ and a cubane-type heterobridged tetranuclear system $[Ni^{II}_4(L^1)_2(HL^1)_2\text{-}(SeCN)_2(H_2O)_2]\cdot C_3H_7NO\cdot 4H_2O$, both of which exhibit fer-

---

[a] Department of Chemistry, University of Calcutta,
92 A. P. C. Road, Kolkata 700 009, India
Fax: +91-33-23519755
E-mail: sm_cu_chem@yahoo.co.in
[b] Institute for Mineralogy and Crystallography,
University of Vienna, Althanstr, 14, 1090 Vienna, Austria
[c] Department of Chemistry, Memorial University of Newfoundland,
St. John's, NL, A1B 3X7, Canada
E-mail: rlucas@mun.ca

Supporting information for this article is available on the WWW under http://dx.doi.org/10.1002/ejic.200900686.

romagnetic interaction. Moreover, the cubane compound is the first example to contain a bis(μ_3-phenoxido)bis(μ_3-alkoxido) bridging moiety and to exhibit an $S_T = 3$ spin ground state in the tetranickel(II) system.[9a] These two compounds, however, do not exhibit any significant electrochemical response. To explore further the heterobridged dinickel(II) compounds with the aim to get ferromagnetically coupled and electrochemically active systems, the reaction between a nickel(II) salt and H_2L^1 in the presence of a base and sodium azide was carried out. Herein, we describe the synthesis, structure, magnetic and electrochemical properties of the product of composition $[Ni^{II}_2(HL^1)_3(\mu_{1,1}\text{-}N_3)]\cdot 3H_2O$ (**1**).

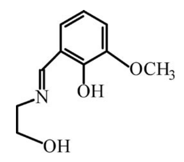

H_2L^1

Scheme 1.

Results and Discussion

Synthesis and Characterization

The dinuclear nickel(II) complex $[Ni^{II}_2(HL^1)_3(\mu_{1,1}\text{-}N_3)]\cdot 3H_2O$ (**1**) is readily obtained in high yield from the reaction of the ligand H_2L^1, nickel(II) perchlorate hexahydrate, triethylamine and NaN_3 in 3:2:6:2 ratio. In **1**, only the phenoxido groups of three ligands are deprotonated.

The IR spectrum of the free ligand H_2L^1 exhibits one strong signal at 1644 cm^{-1} due to a $\nu_{C=N}$ vibration,[13] which appears in a slightly lower region (1636 cm^{-1}) in the dinuclear nickel(II) complex. The presence of azide in **1** is evidenced by the appearance of a very strong band at 2065 cm^{-1}, whereas the stretching for water molecules is observed as a broad band centred at 3392 cm^{-1}.

The poor conductivity of complex **1** (ca. 5 Ω^{-1} cm^2 M^{-1}) in *N,N′*-dimethylformamide (dmf) indicates that the compound remains neutral in solution also. Therefore, azide remains in the inner coordination sphere and expectedly as the bridging ligand. So the μ-phenoxido–$\mu_{1,1}$-N_3 bridging core can be considered as stable in solution.

Description of the Structure of Compound 1

The crystal structure of $[Ni^{II}_2(HL^1)_3(\mu_{1,1}\text{-}N_3)]\cdot 3H_2O$ (**1**) is shown in Figure 1. The structure of **1** reveals that it is a heterobridged μ-phenoxido–$\mu_{1,1}$-azide dinickel(II) compound containing three monodeprotonated $[HL^1]^-$ ligands, in which the phenoxido moiety is deprotonated, one azide anion, which acts as an end-on ($\mu_{1,1}$; EO) bridging ligand, two nickel(II) centres and three water molecules as the solvent of crystallization. Among the three phenolate oxygen atoms of the three $[HL^1]^-$, one [O(1)] acts as a bridging ligand, whereas the other two [O(7) and O(4)] behave as terminal ligands and coordinate to Ni(1) and Ni(2), respectively. Among the three alcohol oxygen atoms, O(8) and O(5) coordinate to Ni(1) and Ni(2), respectively, whereas O(2) remains uncoordinated. The two imino nitrogen atoms, N(1) and N(2), are coordinated to Ni(2), whereas only N(3) is coordinated to Ni(1). Of the three ethereal oxygen atoms, O(3) is coordinated to Ni(1), whereas O(6) and O(9) are uncoordinated. Thus, three ligands are bonded differently to the two metal centres in **1**.

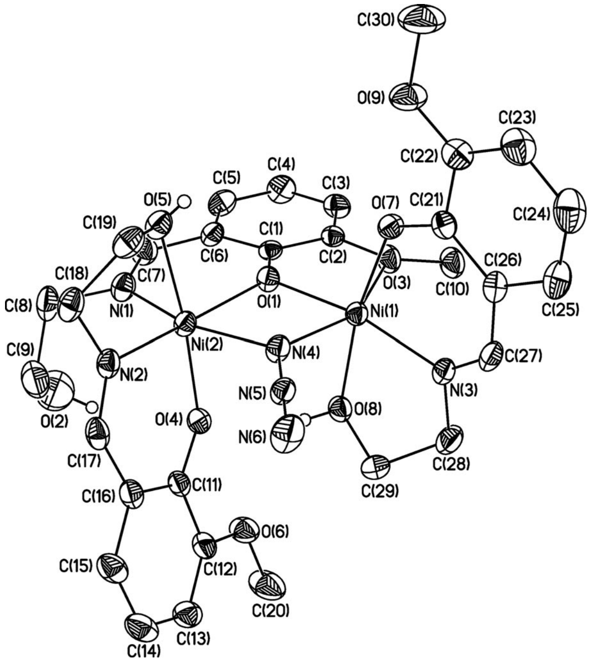

Figure 1. Crystal structure of $[Ni^{II}_2(HL^1)_3(\mu_{1,1}\text{-}N_3)]\cdot 3H_2O$ (**1**). Three water molecules and all hydrogen atoms, except those of three alcohol moieties, are deleted for clarity.

The coordination environment of both the metal ions is distorted octahedral, in which the equatorial planes are provided by O(1)O(3)N(3)N(4) and N(1)N(2)O(1)N(4) for Ni(1) and Ni(2), respectively (Figure 2). Evidently, both the bridging atoms [phenolate oxygen O(1) and azide nitrogen N(4)] occupy two equatorial positions for the two metal ions. The axial positions for both the metal centres are occupied by a phenolate oxygen [O(7) for Ni(1) and O(4) for Ni(2)] and an alcohol oxygen [O(8) for Ni(1) and O(5) for Ni(2)]. The average deviation of the constituent atoms from the least-squares O(1)O(3)N(3)N(4) and N(1)N(2)O(1)N(4) planes are 0.11 and 0.05 Å, respectively, whereas Ni(1) and Ni(2) are displaced by 0.14 and 0.09 Å, respectively, from their corresponding equatorial planes. Clearly, the coordination environment of Ni(1) is more distorted. The dihedral angle between the two equatorial planes [O(1)O(3)N(3)N(4) and N(1)N(2)O(1)N(4)] and between the two planes [Ni(1) O(1)N(4) and Ni(2)O(1)N(4)] involving a metal ion and two bridging atoms are almost identical, 17.9° and 14.1°, respectively.

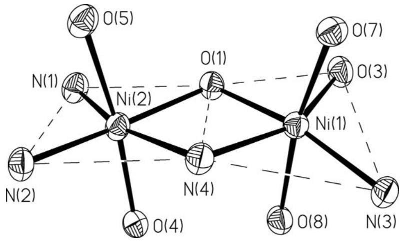

Figure 2. Perspective view of $[Ni^{II}_2(HL^1)_3(\mu_{1,1}\text{-}N_3)]\cdot3H_2O$ (**1**) demonstrating the two equatorial planes. Only two metal ions and the coordinated ligand atoms are shown.

The bond lengths and bond angles in the coordination environment of Ni(1) and Ni(2) are compared in Table 1. The comparison reveals that although the phenoxido bridged Ni–O distances are almost identical [Ni(1)–O(1) 1.993(2) Å, Ni(2)–O(1) 1.990(2) Å], the two azide-bridged Ni–N distances are unequal [Ni(1)–N(4) 2.088(3) Å and Ni(2)–N(4) 2.208(3) Å]. The two Ni–O(alcohol) distances are not much different [Ni(1)–O(8) 2.156(3) Å and Ni(2)–O(5) 2.122(3) Å], as are the two Ni–O(phenolate) distances [Ni(1)–O(7) 1.992(3) Å and Ni(2)–O(4) 2.025(3) Å]. Again, the two imine Ni–N distances are quite similar [Ni(1)–N(3) 1.980(3) Å and Ni(2)–N(2) 1.993(3) Å]. In contrast, the bond length involving the imine nitrogen N(1) to Ni(2) [2.079(3) Å] is longer. The unusually coordinating methoxy oxygen O(3) is rather weakly bonded to Ni(1) [2.250(3) Å]. Considering the six bonds, the bond lengths for Ni(1) and Ni(2) coordination environments lie in the ranges 1.980(3)–2.250(3) and 1.990(2)–2.208(3) Å, respectively. Clearly, as already mentioned, the Ni(2) coordination environment is less distorted. The ranges of the *cis* angles [74.49(10)–104.60(12)° for Ni(1) and 75.96(10)–101.16(13)° for Ni(2)] and *trans* angles [153.11(11)–170.33(11)° for Ni(1) and 165.25(13)–171.44(10)° for Ni(2)] are also indicative of the greater distortion of the Ni(1) coordination environment. The Ni(1)–O(1)–Ni(2) and Ni(1)–N(4)–Ni(2) bridge angles are 106.92(10) and 96.28(12)°, respectively.

It may be mentioned that eight hydrogen bonds involving water molecules of crystallization and $[HL^1]^-$ result in the formation of a self-assembled 1D topology in the title compound (see Figure S1 and Table S1 in the Supporting Information).

Table 1. Selected bond lengths and angles of **1**.

Bond lengths / Å			
Ni(1)–O(7)	1.992(3)	Ni(2)–O(4)	2.025(3)
Ni(1)–O(8)	2.156(3)	Ni(2)–O(5)	2.122(3)
Ni(1)–O(3)	2.250(3)	Ni(2)–N(1)	2.079(3)
Ni(1)–N(4)	2.088(3)	Ni(2)–N(4)	2.208(3)
Ni(1)–O(1)	1.993(2)	Ni(2)–O(1)	1.990(2)
Ni(1)–N(3)	1.980(3)	Ni(2)–N(2)	1.993(3)
Bond angles / °			
O(7)–Ni(1)–O(8)	170.33(11)	O(4)–Ni(2)–O(5)	171.44(10)
O(3)–Ni(1)–N(4)	153.11(11)	N(1)–Ni(2)–N(4)	165.25(13)
O(1)–Ni(1)–N(3)	165.90(12)	O(1)–Ni(2)–N(2)	166.55(13)
O(1)–Ni(1)–O(7)	103.01(11)	O(1)–Ni(2)–O(4)	95.86(10)
O(3)–Ni(1)–O(7)	89.46(11)	N(1)–Ni(2)–O(4)	94.35(13)
N(3)–Ni(1)–O(7)	91.01(12)	N(2)–Ni(2)–O(4)	91.72(12)
N(4)–Ni(1)–O(7)	94.61(12)	N(4)–Ni(2)–O(4)	88.64(12)
O(1)–Ni(1)–O(8)	86.10(12)	O(1)–Ni(2)–O(5)	92.39(11)
O(3)–Ni(1)–O(8)	89.88(11)	N(1)–Ni(2)–O(5)	88.00(13)
N(3)–Ni(1)–O(8)	79.82(13)	N(2)–Ni(2)–O(5)	79.75(13)
N(4)–Ni(1)–O(8)	90.33(12)	N(4)–Ni(2)–O(5)	91.17(12)
O(1)–Ni(1)–O(3)	74.49(10)	O(1)–Ni(2)–N(1)	89.36(12)
O(1)–Ni(1)–N(4)	78.70(11)	O(1)–Ni(2)–N(4)	75.96(10)
O(3)–Ni(1)–N(3)	104.60(12)	N(1)–Ni(2)–N(2)	101.16(13)
N(3)–Ni(1)–N(4)	101.90(13)	N(2)–Ni(2)–N(4)	93.18(12)
Ni(1)–O(1)–Ni(2)	106.92(10)	Ni(1)–N(4)–Ni(2)	96.28(12)

Magnetic Properties

Cryomagnetic behaviour of **1** is shown in Figure 3 in the form of $\chi_M T$ vs. T and χ_M vs. T plots. The $\chi_M T$ value at 300 K is 2.63 cm^3 mol^{-1} K, which is slightly greater than the theoretical $\chi_M T$ value (2.42 cm^3 mol^{-1} K) for two isolated nickel(II) centres with local spins $S_1 = S_2 = 1$ and $g = 2.2$. Upon lowering the temperature from 300 K, $\chi_M T$ remains almost constant up to 120 K. Upon further cooling, $\chi_M T$ increases slowly reaching a maximum value of 2.97 cm^3 mol^{-1} K at 27 K. Below 27 K, $\chi_M T$ decreases rapidly to 0.80 cm^3 mol^{-1} K at 2 K. The profile is indicative of the existence of a weak ferromagnetic interaction between the metal centres. The very sharp decrease in the value of $\chi_M T$ below 27 K may be due to the single-ion anisotropy of the nickel(II) ion. Taking into consideration the exchange interaction, Zeeman splitting (with same g value for the two centres to avoid overparametrization) and single-ion anisotropies, the Hamiltonian for this system is:

$$\mathbf{H} = -2J(\mathbf{S_1}\cdot\mathbf{S_2}) + g\beta\mathbf{S_1}\cdot\mathbf{B} + g\beta\mathbf{S_2}\cdot\mathbf{B} + D_1[S_{Z,1}{}^2] + D_2[S_{Z,2}{}^2]$$

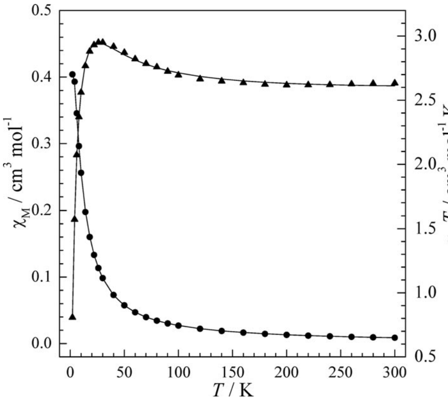

Figure 3. $\chi_M T$ vs. T and χ_M vs. T plots for $[Ni^{II}_2(HL^1)_3(\mu_{1,1}\text{-}N_3)]\cdot3H_2O$ (**1**). Symbols and solid lines represent the observed and calculated data, respectively.

Using this Hamiltonian, the susceptibility data were fitted with JULX software.[14] A fixed temperature-independent paramagnetism of 100×10^{-6} cm^3 per mol of nickel(II) was taken. As shown by the solid lines in Figure 3, a good quality simulation is obtained with $J = 5.0$ cm^{-1}, $g = 2.23$, $D_1 = 29.2$ cm^{-1} and $D_2 = 10.7$ cm^{-1}. If $D_1 = D_2$ is considered, the simulation converges with $J = 3.5$ cm^{-1}, $g = 2.24$, $D_1 = D_2 = 16.8$ cm^{-1}. Comparison of these two simulations in Figures S2 (10–300 K) and S3 (2–35 K; Supporting Information) indicates that significant divergence of calculated data occurs throughout the temperature range if D_1 and D_2 are equal. Therefore, the set of parameter values J = 5.0 cm^{-1}, g = 2.23, D_1 = 29.2 cm^{-1} and D_2 = 10.7 cm^{-1} is taken as the best solution. As the Ni(1) coordination environment is more distorted, it is logical to assign a higher D value (D_1 = 29.2 cm^{-1}) to Ni(1) and a smaller value (D_2 = 10.7 cm^{-1}) to Ni(2).

It may be relevant to compare the g and D values observed for **1** with those of the reported cases. Although the g values in distorted octahedral nickel(II) containing compounds are usually less than or equal to 2.2,[9b,11b–11d,15] larger values like 2.23,[16a] 2.26,[9b,16b] 2.27,[8a] 2.28[10b,11d] and even 2.35,[16b] 2.38[15d] and 2.39[16c] have been observed previously. Regarding the D parameter, there are cases where either D is not taken in simulation or the value of this parameter has been found to be very small.[10b,11d,15b–15d,16a,16b] However, cases are known where larger D values around 10,[11d,15b] 35[15b] and even 45[15b] cm^{-1} have been observed. Clearly, g = 2.23, D_1 = 29.2 cm^{-1} and D_2 = 10.7 cm^{-1} in compound **1** are not unusual.

As already mentioned, heterobridged compounds of 3d metal ions, other than copper(II), are limited. Regarding μ-phenoxido/alkoxido/hydroxido–μ-azide nickel(II) systems, few polymetallic μ-alkoxido–μ-azide $\mathrm{Ni^{II}}_{10}$, $\mathrm{Ni^{II}}_{14}$ and $\mathrm{Ni^{II}}_{12}\mathrm{Na^{I}}_{2}$ clusters,[10] one μ-alkoxido–μ-azide hexanickel(II) compound,[11a] a few μ-alkoxido–μ-azide tetranickel(II) systems,[11b–11e] three μ-phenoxido–μ-azide dinickel(II) compounds[8] and one hexanickel(II) compound[11f] having both μ-alkoxido–μ-azide and μ-carbonato–μ-azide bridging moieties are known. Although magnetic measurements of the $\mathrm{Ni^{II}}_{10}$, $\mathrm{Ni^{II}}_{14}$ and $\mathrm{Ni^{II}}_{12}\mathrm{Na^{I}}_{2}$ clusters have been carried out and high-spin ground states like S_T = 10 or 6 have been observed, it was not possible to determine the magnitude of exchange integrals. However, the exchange integrals in the hexanuclear and tetranuclear systems have been reported, which are listed in Table 2. One metal centre in one of the three μ-phenoxido–μ-azide dinickel(II) compounds is diamagnetic and this compound behaves magnetically like a mononuclear nickel(II) system.[8b] Although the two metal centres in the other two compounds are paramagnetic, magnetic studies of one compound has not been reported,[8b] whereas cryomagnetic measurements of the remaining compound was carried out and the exchange integral of this system is listed in Table 2.[8a]

While considering magnetic exchange interactions in heterobridged systems, the bridge angles for both the exchange pathways should be taken into consideration. It is established that if the Ni–phenoxido–Ni bridge angle is greater than 97°, antiferromagnetic behaviour is expected.[2b] In contrast, the interaction is predicted to be ferromagnetic for the end-on (EO) azide-bridged $\mathrm{Ni^{II}}$ complexes,[5a,12] with J increasing upon increasing the angle, yielding a maximum at 104°.[12] It has also been established theoretically that the extent of ferromagnetic interaction in EO azide-bridged $\mathrm{Ni^{II}}$ complexes decreases linearly with the Ni–N bond lengths.[12] These three governing structural parameters of the μ-alkoxido/phenoxido–μ-azide nickel(II) systems, for which exchange integrals are known, are also listed in Table 2.

The exchange integrals through the μ-alkoxido–μ-azide route in the $\mathrm{Ni^{II}}_4$ and $\mathrm{Ni^{II}}_6$ complexes vary between 1.44 and 10.60 cm^{-1}. However, it is not possible to rationalize these interactions with the structural parameters. The cooperative effect of the other superexchange pathways in these compounds may be a reason not to find any magnetostructural correlation. It will therefore be more relevant to compare the exchange integral observed in the title compound $[\mathrm{Ni^{II}}_2(\mathrm{HL}^1)_3(\mu_{1,1}\text{-}\mathrm{N}_3)]\cdot 3\mathrm{H_2O}$ (**1**) with that of the sole previously reported example of a similar dinickel(II) compound $[\mathrm{Ni^{II}}_2(\mathrm{L}^2)_2(\mu_{1,1}\text{-}\mathrm{N}_3)(\mathrm{N}_3)(\mathrm{H_2O})]\cdot\mathrm{H_2O}$ {**2**; L^2 = $\mathrm{Me_2N(CH_2)_2NCHC_6H_3(O^-)(OCH_3)}$}, the relevant data of which are listed in Table 2.[8a] Although both **1** and **2** are ferromagnetically coupled, the exchange integrals in these two compounds are significantly different; J = 5.0 cm^{-1} for **1** and J = 25.6 cm^{-1} for **2**. In spite of the almost identical values of the two key structural parameters, Ni–O(phenoxido)–Ni (106.9° for **1** and 106.7° for **2**) and Ni–N(azide)–Ni (96.3° for **1** and 96.5° for **2**) bridge angles, the appreciable difference in the magnetic properties is surprising, at least apparently. Again, the Ni–O(phenoxido) bond lengths in the bridging cores of these two compounds are also almost identical; 1.993(2) and 1.990(2) Å for **1** and 1.984(2) and 1.989(2) Å for **2**. Therefore, it seems that the Ni–N(azide) bond lengths may play a crucial role here. The two Ni–N(azide) bond lengths in **2** are almost equal, 2.13 and 2.15 Å. In contrast, these two distances in compound **1** are significantly different, 2.09 and 2.21 Å. As the phenoxido bridge angle (ca. 106°) in both **1** and **2** are greater by 9° than the angle of accidental orthogonality,[2b] the interac-

Table 2. Magnetic and structural parameters of the μ-phenoxido/alkoxido–$\mu_{1,1}$-azide/cyanate nickel(II) compounds.

	Nuclearity	Bridging moiety	J / cm^{-1}	Ni–O–Ni angle / °	Ni–N–Ni angle / °	Ni–O distance / Å	Ni–N distance / Å	Ref.
1	$\mathrm{Ni^{II}}_2$	μ-phenoxido–$\mu_{1,1}$-$\mathrm{N_3}$	5.0	106.9	96.3	1.99, 1.99	2.09, 2.21	this work
2	$\mathrm{Ni^{II}}_2$	μ-phenoxido–$\mu_{1,1}$-$\mathrm{N_3}$	25.6	106.7	96.5	1.98, 1.99	2.13, 2.15	[8a]
3	$\mathrm{Ni^{II}}_2$	μ-phenoxido–$\mu_{1,1}$-NCO	3.3	106.5	94.1	1.98, 1.99	2.11, 2.24	[9a]
4	$\mathrm{Ni^{II}}_2$	μ-phenoxido–$\mu_{1,1}$-NCO	6.2	110.5	96.2	2.00, 2.02	2.02, 2.24	[8a]
5	$\mathrm{Ni^{II}}_4$	μ-alkoxido–$\mu_{1,1}$-$\mathrm{N_3}$	3.5	100.4	102.4	2.10, 2.14	2.07, 2.10	[11b]
6	$\mathrm{Ni^{II}}_4$	μ-alkoxido–$\mu_{1,1}$-$\mathrm{N_3}$	7.3	100.6	101.8	2.10, 2.12	2.08, 2.11	[11c]
7	$\mathrm{Ni^{II}}_4$	μ-alkoxido–$\mu_{1,1}$-$\mathrm{N_3}$	9.4	94.7–99.6	103.2	2.03–2.13	2.06, 2.07	[11d]
8	$\mathrm{Ni^{II}}_4$	μ-alkoxido–$\mu_{1,1}$-$\mathrm{N_3}$	10.6	98.8	97.6, 98.5	2.10–2.12	2.11–2.14	[11e]
9	$\mathrm{Ni^{II}}_6$	μ-alkoxido–$\mu_{1,1}$-$\mathrm{N_3}$	1.44	92.0–93.5	90.0–90.2	2.05–2.06	2.07–2.12	[11a]
10	$\mathrm{Ni^{II}}_6$	μ-alkoxido–$\mu_{1,1}$-$\mathrm{N_3}$	6.1	92.5–94.4	91.2–93.8	2.02–2.14	2.03–2.16	[11f]

tion through the phenoxido bridge should be antiferromagnetic. Therefore, the overall ferromagnetic interaction in **1** and **2** is determined by the extent of ferromagnetic interaction propagated through the azide bridge. According to the azide bridge angle, the ferromagnetic interaction should be almost equal for the two complexes. However, due to one long and one short nickel(II)–azide bond in **1**, the azide bridge propagates less ferromagnetic interaction than that in **2** in which the two nickel(II)–azide bond lengths are almost equal.

In addition to distances and angles involving metal centres and bridging ligands, the dihedral angle (δ_1) between the equatorial planes of the coordination environments may also influence the nature and magnitude of exchange coupling and therefore this parameter in **1** and **2** should be considered. It is known that as this dihedral angle δ_1 increases from 0°, the interaction becomes more ferromagnetic.[1a,6a] The δ_1 values in **1** and **2** are 17.9 and 10.0°, respectively. Therefore, on the basis of δ_1, interaction in **1** should be more ferromagnetic than that in **2**. Clearly, as the reverse order is observed, consideration of dihedral angle between the two equatorial planes strengthens the bridge distance dependency of the exchange integral of **1** and **2**. It may be argued that the dihedral angle (δ_2) between the two planes involving a metal ion and two bridging atoms may also govern the exchange interaction. It is well known that this parameter δ_2 has the significant role to govern the magnetic properties of 3d–4f compounds, because the magnitude of the exchange coupling is dependent on the exchange transfer integral between the lanthanide 5d orbitals and the 3d orbitals of 3d metal ions, with the maximum value to be found when the two planes are coplanar.[2a,17] In contrast, δ_2 is not usually considered to compare the magnetic behaviour of 3d–3d systems. However, the effect of δ_2 on exchange interaction of 3d–3d systems should be similar to that of δ_1, which again strengthens (δ_2 = 14.1° for **1** and 5.9° for **2**; δ_1 = 17.9° for **1** and 10.0° for **2**) the bridge distance dependency of the exchange integral of **1** and **2**.

It is interesting to note that whereas the J values of the two μ-phenoxido–$\mu_{1,1}$-azide dinickel(II) compounds $[Ni^{II}_2(HL^1)_3(\mu_{1,1}\text{-}N_3)]\cdot 3H_2O$ (**1**; J = 5.0 cm^{-1}) and $[Ni^{II}_2(L^2)_2(\mu_{1,1}\text{-}N_3)(N_3)(H_2O)]\cdot H_2O$ (**2**; J = 25.6 cm^{-1}) are significantly different, the extent of ferromagnetic interaction of the two μ-phenoxido–$\mu_{1,1}$-cyanate dinickel(II) compounds $[Ni^{II}_2(HL^1)_3(\mu_{1,1}\text{-}NCO)]\cdot 2H_2O$ (**3**; J = 3.3 cm^{-1}; Table 2)[9a] and $[Ni^{II}_2(L^2)_2(\mu_{1,1}\text{-}NCO)(NCO)(H_2O)]\cdot H_2O$ (**4**; J = 6.2 cm^{-1}; Table 2) are comparatively closer.[8a] Three types of metrical parameters, phenoxido and cyanate bridge angles and metal–cyanate distances, are different for the two compounds (Table 2). The dihedral angle between the two equatorial planes in **3** and **4** are, respectively, 17.5 and 10.3°. The combined effect of these parameters results in weak ferromagnetic interaction in both compounds. Whereas the two metal–azide bond lengths are different and almost equal in **1** and **2**, respectively, the two metal–cyanate bond lengths in both the compounds **3** and **4** are different (2.11 and 2.24 Å for **3**; 2.02 and 2.24 Å for **4**). Moreover, due to the difference in phenoxido and cyanate bridge angles in compounds **3** and **4**, it is not possible to understand the role of a particular parameter in exchange interaction. In contrast, as already discussed, compounds **1** and **2** represent a unique pair demonstrating the role of metal–ligand bridge distance in exchange interaction.

Electrochemistry

The cyclic voltammetric (CV) measurements of **1** were carried out in dmf at 25 °C under a nitrogen atmosphere with the use of glassy carbon and platinum working electrodes for the reduction and oxidation windows, respectively. In the oxidation up to 2000 mV, no electrochemical response was observed. In contrast, in the potential window ranging from 0 to –2000 mV with scan rate of 100 mV s^{-1}, two redox couples are observed. Observing the peak potential values (vide infra), the scan was done in the window ranging from –1000 to –2000 mV. In this cyclic voltammogram (Figure 4), two cathodic responses at –1477 and –1838 mV and, in the return sweep, two anodic peaks at –1685 and –1348 mV were observed. Evidently, the stepwise reductions $Ni^{II}Ni^{II} \rightarrow Ni^{II}Ni^{I}$ and $Ni^{II}Ni^{I} \rightarrow Ni^{I}Ni^{I}$ takes place at –1477 and –1838 mV, respectively, whereas the stepwise oxidations $Ni^{I}Ni^{I} \rightarrow Ni^{I}Ni^{II}$ and $Ni^{I}Ni^{II} \rightarrow Ni^{II}Ni^{II}$ take place at –1685 and –1348 mV, respectively. The $E_{1/2}$ values of these two peaks are –1412 and –1762 mV, whereas the ΔE_p values of these two peaks are 129 and 153 mV, respectively, indicating that both the peaks are quasireversible. It may be mentioned that there is no report of the electrochemical properties of heterobridged compounds related to the title compound.

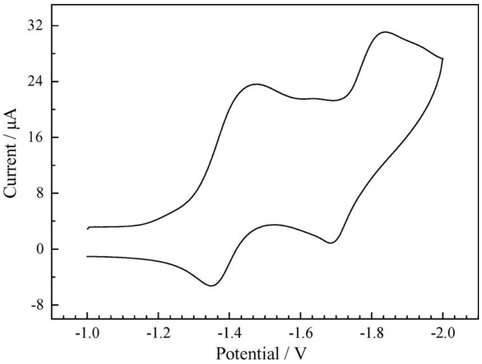

Figure 4. Cyclic voltammogram (–1000 to –2000 mV) of $[Ni^{II}_2(HL^1)_3(\mu_{1,1}\text{-}N_3)]\cdot 3H_2O$ (**1**) in dmf at a scan rate of 100 mV s^{-1}.

Conclusions

The title compound $[Ni^{II}_2(HL^1)_3(\mu_{1,1}\text{-}N_3)]\cdot 3H_2O$ (**1**) is only the second example of a μ-phenoxido/alkoxido/hydroxido–$\mu_{1,1}$-azide dinickel(II) system having magnetic exchange interaction. As the heterobridged compounds of 3d metal ions, other than copper(II), are limited, compound **1** is an important addition in this rare family. Again, as the electrochemical properties of the heterobridged compounds have not been studied previously, the data of cyclic voltammetric measurements of **1** deserves attention; correlation of the reduction potential with structural parameters and the environment of the ligand may be possible from the studies of a few more similar systems. The exchange interaction in **1** involving the heterobridged pathways leads to overall weak ferromagnetic behaviour. The observation of ferromagnetism in **1** shows that the synthetic strategy and ligand design have been successful in achieving ferromagnetically coupled heterobridged complexes.[9a] In spite of the fact that both the phenoxido and azide bond angles and metal–phenoxido bond lengths are equal for the title compound $[Ni^{II}_2(HL^1)_3(\mu_{1,1}\text{-}N_3)]\cdot 3H_2O$ (**1**) and a previously reported analogous system $[Ni^{II}_2(L^2)_2(\mu_{1,1}\text{-}N_3)(N_3)(H_2O)]\cdot H_2O$ (**2**),[8a] the strength of the ferromagnetic interaction in these two compounds is significantly different, which is related to almost-equal versus different metal–azide bond lengths in **2** and **1**, respectively. Evidently, compounds **1** and **2** represent a unique pair demonstrating the role of metal–ligand bridge distance on spin coupling, which is the major outcome of the present investigation.

Experimental Section

Materials and Physical Measurements: All the reagents and solvents were purchased from commercial sources and used as received. The Schiff base ligand (H_2L^1) was synthesized following a reported procedure.[13] Elemental (C, H and N) analyses were performed with a Perkin–Elmer 2400 II analyzer. IR spectra were recorded in the region 400–4000 cm^{-1} with a Perkin–Elmer RXIFT spectrophotometer with samples as KBr disks. Cyclic voltammetric (CV) measurements were done by using a Bioanalytical System EPSILON electrochemical analyzer. The concentration of the supporting electrolyte, tetraethylammonium perchlorate (TEAP) was 0.1 M, whereas that of complex **1** was 1 mM. Cyclic voltammetric measurements were carried out in dimethylformamide solution with a three-electrode assembly comprising a glassy carbon disk working electrode, a platinum auxiliary electrode and an aqueous Ag/AgCl reference electrode. The reference electrode was separated from the bulk solution by using a TEAP salt bridge in acetonitrile. Molar conductivity (Λ_M) of a 1 mM solution in dmf of **1** was measured at 25 °C with a Systronics conductivity bridge. Variable-temperature magnetic susceptibility measurements at fixed field strength of 1 T were carried out with a Quantum Design MPMS SQUID magnetometer. Diamagnetic corrections were estimated from the Pascal constants.

$[Ni^{II}_2(HL^1)_3(\mu_{1,1}\text{-}N_3)]\cdot 3H_2O$ (1): To a stirred *N,N′*-dimethylformamide (dmf) solution (5 mL) of H_2L^1 (0.195 g, 1 mmol) was added dropwise a dmf solution (3 mL) of nickel(II) perchlorate hexahydrate (0.250 g, 0.68 mmol), and to the resulting yellowish green solution was added dropwise a dmf solution (2 mL) of triethylamine (0.202 g, 2 mmol). The colour of the solution changed to deep green. After 1 h, an aqueous solution (5 mL) of NaN_3 (0.045 g, 0.68 mmol) was added dropwise to the stirred solution. After stirring for an additional 2 h, the deep green solution was filtered to remove any suspended particles and water (10 mL) was added to it. The solution was kept at room temperature. After 2 d, a green crystalline compound that deposited was collected by filtration and washed with water. Recrystallization from dmf/water yielded a green crystalline compound containing diffraction-quality single crystals. Yield: 0.207 g (78 %). $C_{30}H_{42}N_6Ni_2O_{12}$ (796.11): calcd. C 45.26, H 5.32, N 10.56; found C 45.32, H 5.35, N 10.51. IR (KBr): $\tilde{\nu}$ = 3392 (w, ν_{water}), 2065 (vs, ν_{azide}), 1636 (vs, $\nu_{C=N}$) cm^{-1}.

Crystal Structure Determination: The crystallographic data of $[Ni^{II}_2(HL^1)_3(\mu_{1,1}\text{-}N_3)]\cdot 3H_2O$ (**1**) are listed in Table 3. Single-crystal X-ray intensity data of the title compound were collected at 293 K with a Nonius Kappa diffractometer with a CCD area detector, using 152 frames with ϕ- and *ω*-increments of 2° and a counting time of 80 s per frame. The crystal-to-detector-distance was 28 mm. The reflection data were processed with the Nonius program suite DENZO-SMN and corrected for Lorentz, polarization, background and absorption effects.[18a,18b] The crystal structure was determined by direct methods and subsequent Fourier and difference Fourier syntheses, followed by full-matrix least-squares refinements on F^2 using SHELXL-97.[18c,18d] All the hydrogen atoms except those of the water molecules [O(10), O(11) and O(12)] were inserted at calculated positions with isotropic thermal parameters. All the hydrogen atoms were refined freely. Using anisotropic treatment of the non-H atoms and unrestrained isotropic treatment of the H atoms, the refinement converged at an *R* value $[I > 2\sigma(I)]$ of 0.0534. CCDC-735096 (for **1**) contains the supplementary crystallographic data for this paper. These data can be obtained free of charge from The Cambridge Crystallographic Data Centre via www.ccdc.cam.ac.uk/data_request/cif.

Table 3. Crystallographic data for **1**.

Formula	$C_{15}H_{21}N_3O_6Ni$
Formula weight	398.06
Crystal colour	green
Crystal system	triclinic
Space group	$P\bar{1}$
a / Å	10.127(2)
b / Å	11.514(2)
c / Å	15.328(3)
α / °	91.60(3)
β / °	96.11(3)
γ / °	95.50(3)
V / Å^3	1767.6(6)
Z	4
Temperature / K	293(2)
$D_{calcd.}$ / g cm^{-3}	1.496
μ / mm^{-1}	1.134
$F(000)$	832
2θ / °	8.18–54.92
Reflections collected	12622
Independent reflections	7984
[R_{int}]	[0.0321]
Absorption correction	multiscan
T_{min}	0.9351
T_{max}	0.9561
Index ranges	$-13 \le h \le 13$
	$-14 \le k \le 14$
	$-19 \le l \le 18$
R_1[a]/wR_2[b] $[I > 2\sigma(I)]$	0.0534/0.1202
R_1[a]/wR_2[b] (all data)	0.1036/0.1411

[a] $R_1 = [\Sigma||F_0| - |F_c||/\Sigma|F_0|]$. [b] $wR_2 = [\Sigma w(F_0^2 - F_c^2)^2/\Sigma w F_0^4]^{1/2}$.

Supporting Information (see footnote on the first page of this article): Self-assembled 1D topology in the title compound.

Acknowledgments

Financial support from the Department of Science and Technology, the Government of India (SR/S1/IC-12/2008) and Centre for Research in Nanoscience and Nanotechnology, University of Calcutta is gratefully acknowledged. S.H. and A.J. are thankful to the Council for Scientific and Industrial Research, and R.K. is thankful to the Centre for Research in Nanoscience and Nanotechnology, University of Calcutta, for providing fellowships. Dr. Konstantin Shuvaev, Memorial University of Newfoundland, is acknowledged for collection of the variable-temperature magnetic data.

---

[1] a) O. Kahn, *Molecular Magnetism*, VCH Publications, New York, **1993**; b) R. D. Willet, D. Gatteschi, O. Kahn (Eds.), *Magneto-Structural Correlations in Exchange Coupled Systems*, Reidel, Dordrecht, **1985**; c) C. J. O'Connor (Ed.), *Research Frontiers in Magnetochemistry*, World Scientific, Singapore, **1993**; d) C. T. Chen, K. S. Suslick, *Coord. Chem. Rev.* **1993**, *128*, 293–322.

[2] a) R. Koner, H.-H. Lin, H.-H. Wei, S. Mohanta, *Inorg. Chem.* **2005**, *44*, 3524–3536; b) K. K. Nanda, L. K. Thompson, J. N. Bridson, K. Nag, *J. Chem. Soc., Chem. Commun.* **1994**, 1337–1338; c) M. I. Arriortua, R. Cortés, J. L. Mesa, L. Lezama, T. Rojo, G. Villeneuve, *Transition Met. Chem.* **1988**, *13*, 371–374.

[3] a) E. Ruiz, J. Cirera, J. Cano, S. Alvarez, C. Loose, J. Kortus, *Chem. Commun.* **2008**, 52–54; b) J. Tercero, C. Diaz, J. Ribas, J. Mahía, M. Maestro, X. Solans, *J. Chem. Soc., Dalton Trans.* **2002**, 2040–2046; c) A. Figuerola, C. Diaz, M. S. El Fallah, J. Ribas, M. Maestro, J. Mahía, *Chem. Commun.* **2001**, 1204–1205; d) A. A. Lozano, M. Sáez, J. Pérez, L. García, L. Lezama, T. Rojo, G. López, G. García, M. D. Santana, *Dalton Trans.* **2006**, 3906–3911.

[4] a) R. Winpenny (Ed.), *Single-Molecule Magnets and Related Phenomena*, Springer, Berlin, **2006**; b) J. S. Miller (Ed.), *Extended Linear Chain Compounds*, Plenum, New York, **1983**, vol. III; c) D. Gatteschi, O. Kahn, J. S. Miller, F. Palacio (Eds.), *Magnetic Molecular Materials*, Kluwer Academic Publishers, Dordrecht, **1991**; d) D. B. Amabilino, J. Veciana in *Magnetism*: *Molecules to Materials II* (Eds.: J. S. Miller, M. Drillon), Wiley-VCH, Weinheim, **2001**, pp. 1–60; e) H. Iwamura, K. Inoue in *Magnetism*: *Molecules to Materials II* (Eds.: J. S. Miller, M. Drillon), Willey-VCH, Weinheim, **2001**, pp. 61–108.

[5] a) J. Ribas, A. Escuer, M. Monfort, R. Vicente, R. Cortés, L. Lezama, T. Rojo, *Coord. Chem. Rev.* **1999**, *193–195*, 1027–1068; b) M. Verdaguer, A. Bleuzen, V. Marvaud, J. Vaissermann, M. Seuleiman, C. Desplanches, A. Scuiller, C. Train, R. Garde, G. Galley, C. Lomenech, I. Rosenman, P. Veillet, C. Cartier, F. Villain, *Coord. Chem. Rev.* **1999**, *190–192*, 1023–1047; c) G. Rajaraman, M. Murugesu, E. C. Saudo, M. Soler, W. Wernsdorfer, M. Helliwell, C. Muryn, J. Raftery, S. J. Teat, G. Christou, E. K. Brechin, *J. Am. Chem. Soc.* **2004**, *126*, 15445–15457; d) D. Venegas-Yazigi, E. Ruiz, J. Cano, S. Alvarez, *Dalton Trans.* **2006**, 2643–2646; e) T. C. Stamatatos, V. Nastopoulos, A. J. Tasiopoulos, E. E. Moushi, W. Wernsdorfer, G. Christou, S. P. Perlepes, *Inorg. Chem.* **2008**, *47*, 10081–10089; f) T. C. Stamatatos, D. Foguet-Albiol, S.-C. Lee, C. C. Stoumpos, C. P. Raptopoulou, A. Terzis, W. Wernsdorfer, S. O. Hill, S. P. Perlepes, G. Christou, *J. Am. Chem. Soc.* **2007**, *129*, 9484–9496.

[6] a) Y.-C. Chou, S.-F. Huang, R. Koner, G.-H. Lee, Y. Wang, S. Mohanta, H.-H. Wei, *Inorg. Chem.* **2004**, *43*, 2759–2761; b) V. McKee, J. V. Dagdigian, R. Bau, C. A. Reed, *J. Am. Chem. Soc.* **1981**, *103*, 7000–7001; c) W. Mazurek, B. J. Kennedy, K. S. Murray, M. J. O'Connor, J. R. Rodgers, M. R. Snow, A. G. Wedd, P. R. Zwack, *Inorg. Chem.* **1985**, *24*, 3258–3264; d) Y. Nishida, S. Kida, *J. Chem. Soc., Dalton Trans.* **1986**, 2633–2640; e) T. N. Doman, D. E. Williams, J. F. Banks, R. M. Buchanan, H.-R. Chang, R. J. Webb, D. N. Hendrickson, *Inorg. Chem.* **1990**, *29*, 1058–1062.

[7] a) T. Sato, W. Mori, Y. Xie, N. Kanehisa, Y. Kai, M. Fuji, S. Goto, E. Nagai, Y. Nakao, *Inorg. Chim. Acta* **2006**, *359*, 2271–2274; b) G. Ambrosi, P. Dapporto, M. Formica, V. Fusi, L. Giorgi, A. Guerri, M. Micheloni, P. Paoli, R. Pontellini, P. Rossi, *Dalton Trans.* **2004**, 3468–3474; c) A. K. Boudalis, J.-M. Clemente-Juan, F. Dahan, J.-P. Tuchagues, *Inorg. Chem.* **2004**, *43*, 1574–1586; d) R. Bouwman, P. Evans, R. A. G. de Graaf, H. Kooijman, R. Poinsot, P. Rabu, J. Reedijk, A. L. Spek, *Inorg. Chem.* **1995**, *34*, 6302–6311; e) J. M. Clemente-Juan, C. Mackiewicz, M. Verelst, F. Dahan, A. Bousseksou, Y. Sanakis, J.-P. Tuchagues, *Inorg. Chem.* **2002**, *41*, 1478–1491; f) M. G. Barandika, Z. Serna, R. Cortés, L. Lezama, T. Rojo, M. K. Urtiaga, M. I. Arriortua, *Chem. Commun.* **2001**, 45–46.

[8] a) S. K. Dey, N. Mondal, M. S. E. Fallah, R. Vicente, A. Escuer, X. Solans, M. Font-Barda, T. Matsushita, V. Gramlich, S. Mitra, *Inorg. Chem.* **2004**, *43*, 2427–2434; b) S. Uozumi, H. Furutachi, M. Ohba, H. Ōkawa, D. E. Fenton, K. Shindo, S. Murata, D. J. Kitko, *Inorg. Chem.* **1998**, *37*, 6281–6287.

[9] a) S. Hazra, R. Koner, P. Lemoine, E. C. Sañudo, S. Mohanta, *Eur. J. Inorg. Chem.* **2009**, 3458; b) A. Roth, A. Buchholz, M. Rudolph, E. Sch6tze, E. Kothe, W. Plass, *Chem. Eur. J.* **2008**, *14*, 1571–1573.

[10] a) G. Aromí, S. Parsons, W. Wernsdorfer, E. K. Brechin, E. J. L. McInnes, *Chem. Commun.* **2005**, 5038–5040; b) T. C. Stamatatos, K. A. Abboud, S. P. Perlepes, G. Christou, *Dalton Trans.* **2007**, 3861–3863.

[11] a) M.-L. Tong, M. Monfort, J. M. C. Juan, X.-M. Chen, X.-H. Bu, M. Ohba, S. Kitagawa, *Chem. Commun.* **2005**, 233–235; b) D.-Y. Wu, W. Huang, W.-J. Hua, Y. Song, C.-Y. Duan, S.-H. Li, Q.-J. Meng, *Dalton Trans.* **2007**, 1838–1845; c) Z. E. Serna, L. Lezama, M. K. Urtiaga, M. I. Arriortua, M. G. Barandika, R. Cortés, T. Rojo, *Angew. Chem. Int. Ed.* **2000**, *39*, 344–347; d) Z. E. Serna, M. G. Barandika, R. Cortés, M. K. Urtiaga, G. E. Barberis, T. Rojo, *J. Chem. Soc., Dalton Trans.* **2000**, 29–34; e) J. Ribas, M. Monfort, R. Costa, X. Solans, *Inorg. Chem.* **1993**, *32*, 695–699; f) A. N. Georgopoulou, C. P. Raptopoulou, V. P. Rafael Ballesteros, B. Abarca, A. K. Boudalis, *Inorg. Chem.* **2009**, *48*, 3167–3176.

[12] E. Ruiz, J. Cano, S. Alvarez, P. Alemany, *J. Am. Chem. Soc.* **1998**, *120*, 11122–11129.

[13] S. Hazra, S. Majumder, M. Fleck, S. Mohanta, *Polyhedron* **2008**, *27*, 1408–1414.

[14] E. Bill, *JULX 1.4: A Program for Simulation of Molecular Magnetic Data*, Mülheim/Ruhr26, Germany.

[15] a) J. Cano, G. De Munno, F. Lloret, M. Julve, *Inorg. Chem.* **2000**, *39*, 1611–1614; b) S. Demeshko, G. Leibeling, W. Maringgele, F. Meyer, C. Mennerich, H.-H. Klauss, H. Pritzkow, *Inorg. Chem.* **2005**, *44*, 519–528; c) M. A. Halcrow, J. C. Huffman, G. Christou, *Angew. Chem. Int. Ed. Engl.* **1995**, *34*, 889–891; d) M. Monfort, I. Resino, M. S. El Fallah, J. Ribas, X. Solans, M. Font-Bardia, H. Stoeckli-Evans, *Chem. Eur. J.* **2001**, *7*, 280–287.

[16] a) C. S. Hong, Y. Do, *Angew. Chem. Int. Ed.* **1999**, *38*, 193–195; b) J. Ribas, M. Monfort, B. K. Ghosh, X. Solans, *Angew. Chem. Int. Ed. Engl.* **1994**, *33*, 2087–2089; c) J. Ribas, M. Monfort, I. Resino, X. Solans, P. Rabu, F. Maingot, M. Drillon, *Angew. Chem. Int. Ed. Engl.* **1996**, *35*, 2520–2522.

[17] a) I. Ramade, O. Kahn, Y. Jeannin, F. Robert, *Inorg. Chem.* **1997**, *36*, 930–936; b) J.-P. Costes, F. Dahan, A. Dupuis, *Inorg. Chem.* **2000**, *39*, 165–168; c) R. Koner, G.-H. Lee, Y. Wang, H.-H. Wei, S. Mohanta, *Eur. J. Inorg. Chem.* **2005**, 1500–1505.

[18] a) Z. Otwinowski, W. Minor, *Methods Enzymol.* **1997**, *276*, 307–326; b) V. N. Sonar, M. Venkatraj, S. Parkin, P. A. Crooks, *Acta Crystallogr., Sect. C* **2007**, *63*, o493–o495; c) G. M. Sheldrick, *Acta Crystallogr., Sect. A* **2008**, *64*, 112–122; d) G. M. Sheldrick, *SHELXL-97*: *Crystal Structure Refinement Program*, University of Göttingen, Göttingen, Germany, **1997**.

Received: July 21, 2009